COMPOSITE STEEL-CONCRETE BRIDGE: ANALYSIS WITH FINITE ELEMENT METHOD

Rebeca Jéssica Schmitz

Inácio Benvegnu Morsch

rebeca.schmitz@ufrgs.com

morsch@ufrgs.com

Affiliation

Centro de Mecânica Computacional e Aplicada (CEMACOM) - UFRGS

Avenida Osvaldo Aranha, 99, 90040-020, Porto Alegre, Rio Grande do Sul, Brasil

Abstract. *Composite steel-concrete components are usually used in bridges structural elements: in this research an application in bridge structures is studied. The goal of this work is to analyze the behavior of a bridge structure designed by a normative code. The bridge´s design was done using a simplified model in ANSYS software to analyze how the actions and some normative references, such as NBR8800, EUROCODE 4 and AASTHO, apply to the elements design. In this research, it is used a more complex model developed in ANSYS, using the software customization for include the concrete behavior. In the first analysis it was verified the effects of the environmental conditions on concrete creep and shrinkage along ten years, considering nine different situations and combining temperature and air humidity. Another analysis was about the level of stress on the structure components considering all actions combined on two cases for the permanent load: young structure (without time effects) and considering the predicted time effects, which were verified on the earlier analysis. Comparing these obtained values with the values adopted in the design, there is a little difference on each one, but the design is still safe.*

Keywords: *Steel-concrete bridges; Finite element method; ANSYS customization*

INTRODUCTION

The finite element method is a good tool to do refined analysis of structures and its efficiency was proven by many studies. Other benefit is that exist some commercial softwares that use this method so is not necessary to developed a new one. In this work it was used the ANSYS software, which has many elements types and material models available for the users. The analysis is about a composite steel-concrete bridge, which was not built and the design was done in a previous academic work, but considering all normative design.

The model for the bridge was based on a model for composite steel-concrete beam that was validated in Schmitz (2017). This researcher considered some important previous works about composite beams for the developed. Tamayo et al. (2015) developed a software to analyze composite beams considering effects generated by short-term loads, like plastic deformation, cracking and crushing of concrete. The improvements of Dias et al. (2015) and Moreno et al. (2016) on the same software brought the possibility to verify the effects generated by long-term loads.

Another two researchers gave important contributions for the present model. Kotinda (2006) and Queiroz et al. (2007) modelled composite beams in ANSYS to analyze effects of short-term loads, and each one considered a different way to model the steel-concrete interface. Kotinda (2006) used contact elements and beam elements (beam189) represented the connectors. Queiroz et al. (2007) have represented this interface using only spring elements (combina39) for the connectors.

The present job analyze a composite steel-concrete bridge considering effects of short and long-term loads. The analysis contemplate the deferred effects considering some environmental conditions, verifications about stress level and effective width in a young structure (without deferred effects) and in a structure with ten years of service.

1 FINITE ELEMENT MODEL

1.1 Material models

In a composite beam there are two materials to be modelled: steel and concrete. However, steel is present in three ways on the structure: “I” profile (structural steel), the shear connectors, and the reinforcements inside the concrete slab. Considering the different characteristics by each one, it was adopted three different models.

The structural steel, that can be “I” profiles or box girders, was modeled like an elastoplastic material with a nonlinear ha rdening. The constitutive model is the same implemented by Gattesco (1999) illustrated in Fig. 1, considering the Eq. 1 for the hardening branch:

$$\sigma_s = f_{s\gamma} + E_{sh} \cdot \left(\varepsilon_s - \varepsilon_{sh}\right) \cdot \left[1 - E_{sh} \cdot \frac{\varepsilon_s - \varepsilon_{sh}}{4 \cdot \left(f_{su} - f_{s\gamma}\right)}\right] \tag{1}$$

Proceedings of the XXXVIII Iberian Latin-American Congress on Computational Methods in Engineering
P.O. Faria, R.H. Lopez, L.F.F. Miguel, W.J.S. Gomes, M. Noronha (Editores), ABMEC, Florianópolis, SC, Brazil, November 5-8, 2017.

where $f_{s\gamma}$ is the yield stress and f_{su} is the ultimate stress; ε_s and ε_{sh} represent the current strain and the strain on the beginning of the hardening branch, respectively; E_{sh} is the tangent modulus of elasticity on the beginning of the hardening branch, adopted equal to 350 kN/cm².

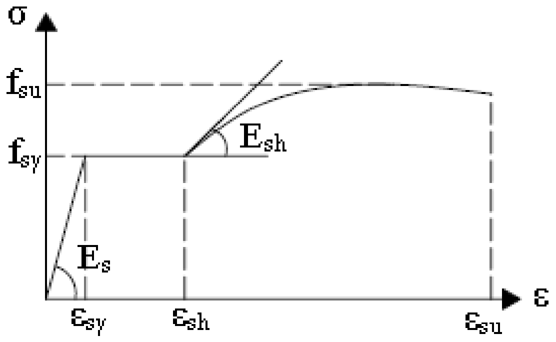

Figure 1. Structural steel model (Gattesco, 1999)

The reinforcement steel was modelled near the perfect elastoplastic behavior, being considered a small hardening (1/1000) to prevent convergence problems. The structural steel used in “I” profiles and the reinforcement steel were inserted using the material type MISO (Multilinear Isotropic Hardening) available in ANSYS. The MISO model uses von Mises criterion for plasticity.

The shear connectors were modelled according to the push out curve generated by a test, like presented in Fig. 2. The curve is defined by the two parameters "a" and "b". So on this case the steel behavior is represented by the specific case of connectors. The curve is used to define the stiffness that can be tangent or secant, but ANSYS always adopts the tangent stiffness. Another important information of this curve is about the failure, if the calculated deformation represents a bigger displacement than the limit of the graphic, the connector broke. These behavior can be modelled by real constants of a nonlinear spring element (combin39), which is presented on the next item.

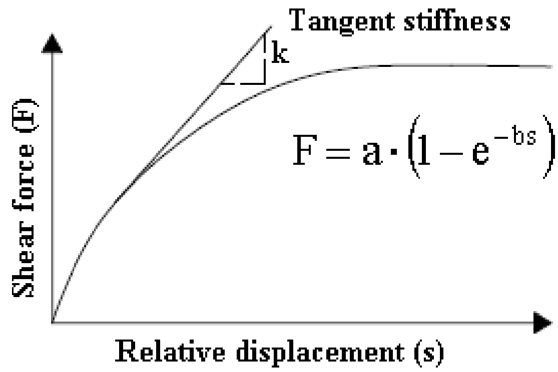

Figure 2. Connectors’ behavior (push out curve)

The other material implemented was concrete, that is divided considering load characterisitics. When concrete is subjected to short-term loads, it is analyzed the elastoplastic deformation, crushing in compression and cracking until failured for tension. Besides that when concrete is subjected to long-term loads, it can be observed deformation increase along the time, generated by deferred effects, such as creep and shrinkage.

First is presented the behavior for short-term loads. Concrete has a really different behavior considering compression and tension. In compression it is modeled like a elastoplastic material according the Fig. 3 of the Model Code 2010 by Féderation Internationale du Béton – FIB (2012). The von Mises criterion is adopted as the plasticity criterion, but for the crushing is considered the Ottosen criterion in stress and the deformation limit presented on the graphic.

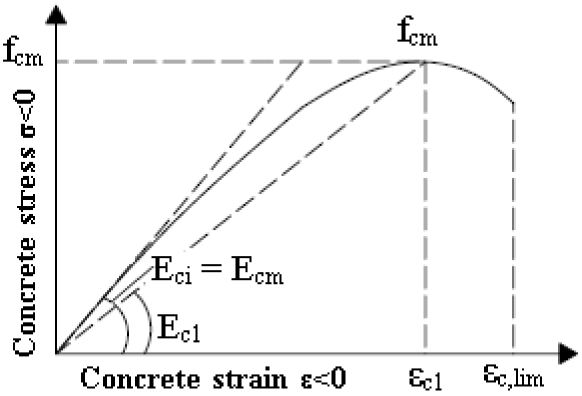

Figure 3. Concrete behavior in compression (FIB, 2012)

Concrete in tension is a fragile material, so until the formation of the first crack the behavior is elastic, when the first crack comes up, concrete demonstrates a big loss of stiffness but still contributing for the structure stiffness. This phenomenon is known by tension stiffening, and is represented numerically by a linear softening, like in Fig. 4. The adopted criterion to verify the cracking is also the Ottosen.

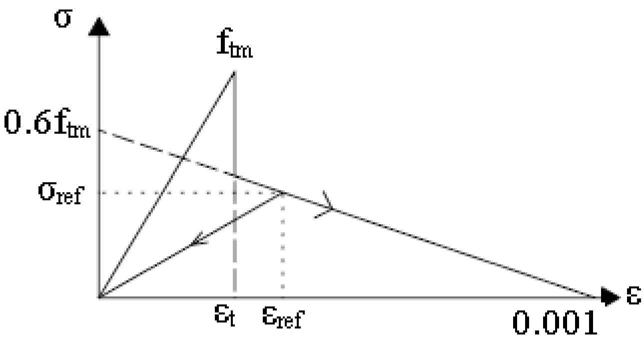

Figure 4. Concrete behavior in tension (Martinelli, 2003)

Another information is about the transverse stiffness modulus , that does not become zero, the roughness of the crack surface still allows to transmit some shear, so this module is multiplied by the factor β_f according to Eq. 2:

$$\beta_f = 1 - \left(\frac{\varepsilon_T}{0.005} \right)^{k_1} \quad (2)$$

where ε_T is a fictitious deformation perpendicular to the crack, and k_1 is an undimensional parameter usually between 0.3 and 1, herein adopted equal to 0.3, according to Martinelli (2003), who implemented this relation.

One of the deferred effects to be considered is shrinkage. This phenomenon is caused by the loss of water that occur mainly during the first ages because of the drying of the water remained by cement reactions in pores. The other phenomenon is related with the stress, and is named creep. Concrete is a material that even subjected to constant load, demonstrates a growing deformation. Many theories present formulation to evaluate these deformations. On the present work was adopted two codes: Comité Euro-International du Béton (1993) and Féderation Internationale du Béton (2012). However, to analyze creep with some loads acting on the structure on different ages was adopted the Solidification Theory of Bazant e Prasannan (1988). For the correct use of these theories is important that the applied stress does not overcome 40% of concrete compressive strength considering its age when the load are applied.

The Solidification Theory considered that the aging of concrete can be represented in a function related by the cement paste volume, because the aggregate has allways the same volume. Therefore, the theory separates the creep function on two parts: a function of volume that gives the aging and the other part that is adjusted by a Kelvin chain, with constants parameters for the springs and dampers. Eq. 3 summarize this theory:

$$J(t,t') = \frac{1}{E(t')} + \frac{\gamma(t,t')}{V(t)} \tag{3}$$

Where J(t,t’) is the creep function, for a concrete current age t and the age of concrete at loading t’. E(t’) is the tangent modulus of elasticity at the age t’, and γ(t,t’) is the creep without aging (adjusted by Kelvin chain), so V(t) is the function of volume related by current age.

To implement this complex model for concrete it was necessary to customize the software using the UserMat tool, designated to program any material, according to the user needs. All details about this process of implementation and validation can be read in Schmitz (2017).

1.2 Finite elements adopted

To represent the steel section of the composite beam (“I” profile or box girder) was chosen a shell element, shell181, and the concrete slab was modeled with a solid tridimensional element, solid186. Considering the possibility of reinforced concrete, the reinforcement is modeled with reinf264. Lastly, the shear connectors are modeled with a nonlinear spring, combin39. So all adopted elements are in ANSYS library, and they are presented below, but there are more information about them in ANSYS manual.

According ANSYS Inc. (2010), the element shell181 has four nodes (see Fig. 5), and linear interpolation functions. It was considered that this element has membrane and bending stiffness, in consequence each node has six degrees of freedom (three translations: UX, UY, UZ; three rotations: ROTX, ROTY, ROTZ). The element is based on the Midlin-Reissner theory, which is proper to thin to moderately thick shell structures. For each different kind of shell181 elements it is necessary to define the thickness, the material model, the angle (in degrees) for orientation, the number of integration points through the thickness. On this study, the material of the shell elements is elastoplastic, therefore it is necessary to use at least five integration points.

Solid186 is a tridimensional element with twenty nodes, so it has a quadratic interpolation functions, like presented in Fig. 5. On this situation, the use of a quadratic element brings benefits because the material behavior programmed has many nonlinearities, because of this makes the convergence process difficult. It is necessary to highlight that this element does not accept the ready model “Concrete” of ANSYS. Each node has three degrees of freedom that are the translations in directions X, Y, Z.

The element solid186 can be divided in layers, but it was used in a homogenous mode, and the reinforcements are included with other type of element: reinf264. This element is ideal to model reinforcement because it has only axial stiffness and can be located in any direction inside the solid186 element. The elements of reinforcement share the nodes with its base element, so do the connectivity.

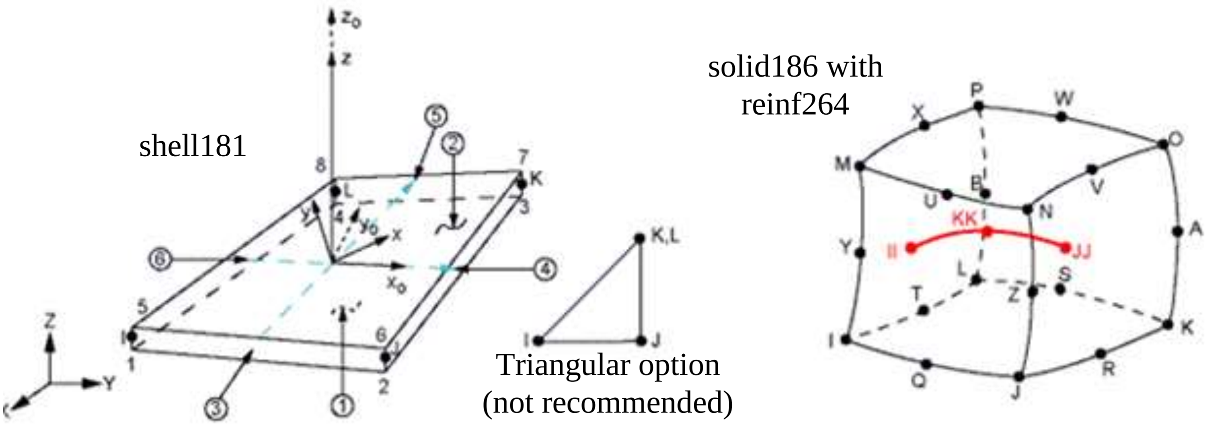

Figure 5. Concrete slab and steel profile finite elements used to model the composite beam (ANSYS Inc, 2010)

The model for shear connectors was based on Queiroz et al. (2007) and it is summarized in Fig. 6. Each element represents one connector, and each element is formed by two coincident nodes. Observing the Fig. 6 it is possible to see a small distance between the nodes that form the element. This distance is equal to half of the top flange thickness and does not compromises the accuracy of results. The element has one degree of freedom on the slip direction, so in the other two direction it is necessary to put the condition of coupled nodes to guarantee the equilibrium of the structure.

The element combin39 is a nonlinear spring, that has torsional or longitudinal mode, so it can be used considering the relation of shear and slip or torsion and rotation. In this case the longitudinal mode is used, so the stiffness of the element is given by the push out curve. Combin39 does not have any mass or damping, and is defined only by the element options and the real constants. It is available forty real constants reserved to insert the points of the curve of shear versus slip. So it is possible to inform twenty points of this curve, and it is necessary to inform the slip and the shear for each point.

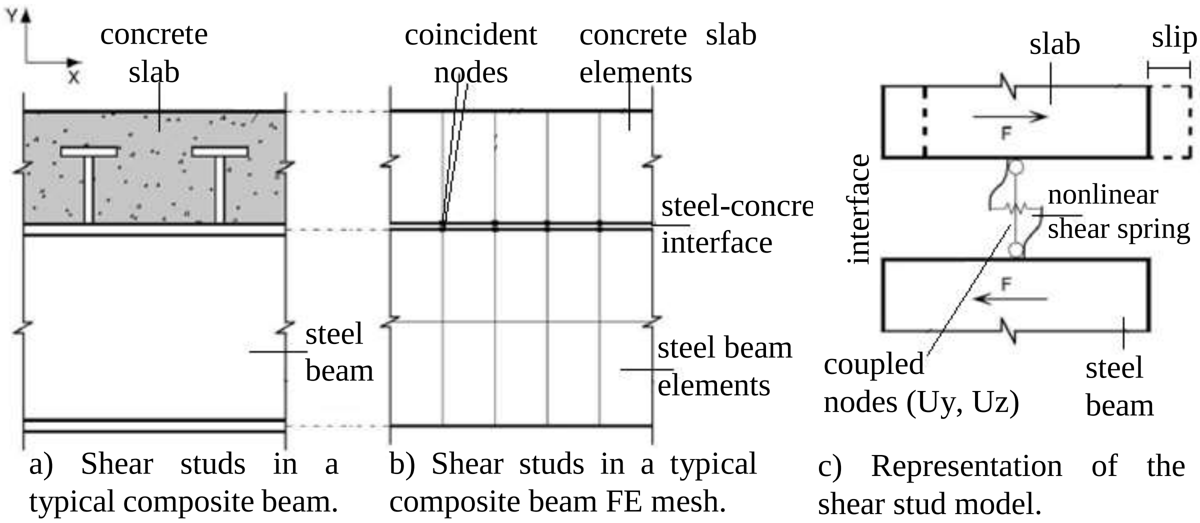

Figure 6. Connectors' model (adapted from Queiroz et al., 2007)

2 BRIDGE: MODEL AND ANALYSIS

2.1 Bridge analyzed

The chosen bridge for analysis has only one span with 30 m and is a simply supported structure. The deck is composed by 8 principal composite beams spaced 1.83 m and five lines of transverse steel beams (diaphragms) every 7.50 m. The slab has a 0.25 m of thickness in reinforced concrete. Fig. 7 presents the bridge that has two lanes and a sidewalk on each side with symmetry in its transverse section.

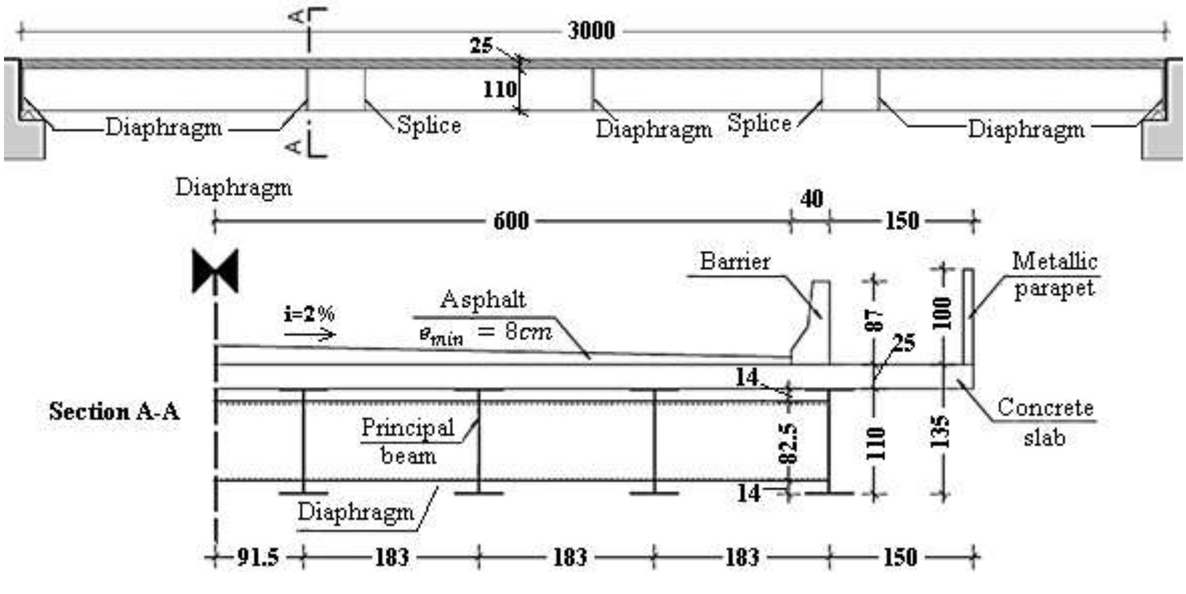

Figure 7. Bridge dimensions (cm)

The composite beams are composed by I profiles with dimensions presented in Fig 8. The dimensions of the transverse beams (diaphragms) are also shown in Fig 8. The structural steel is COR500, in order to prevent corrosion by environmental attack. The connectors are in groups of three spaced by 0.505 m along the span. The slab is composed by pre-fabricated elements with resistance equal to 45 MPa and steel CA-50 for the reinforcement. All materials properties are shown in Table 1. The design of all components of the bridge were made in a previous work based on the codes NBR 8800 (Associação Brasileira de Normas Técnicas – ABNT, 2008), AASHTO (American Association of State Highway and Transport Officials, 2012) and EUROCODE 4 (European Commitee for Standardization, 2005).

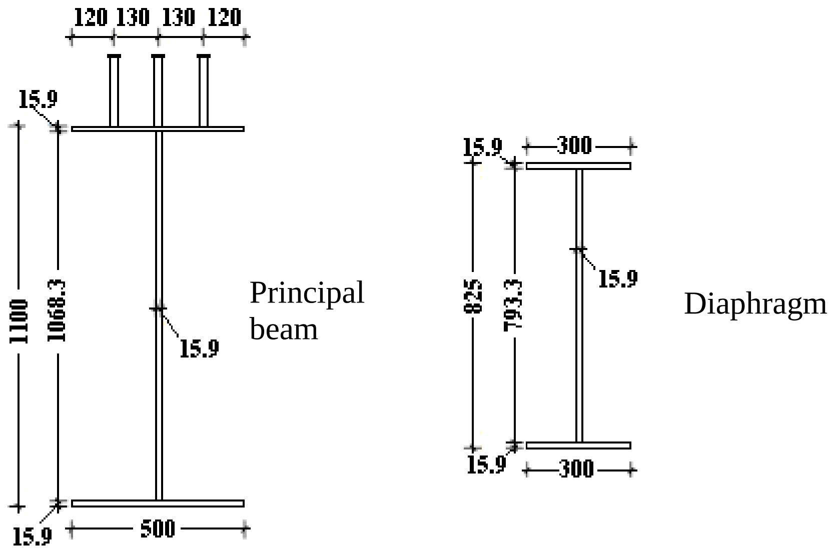

Figure 8. Beams dimensions (millimeters)

Table 1. Materials proprieties

Steel COR500		**Concrete**	
Specific weight (kN/cm³)	7.70E-05	Specific weight (kN/cm³)	2.50E-05
Modulus of elasticity (kN/cm²)	2.00E+04	Poisson’s ratio	0.2
Poisson’s ratio	0.3	Characteristic strength (kN/m²)	4.5
Yield stress (kN/cm²)	37	Type of cement	42.5 R, 52.5 N, 52.5 R
Ultimate stress (kN/cm²)	45	Type of aggregate	quartzite
Yielding	inexistent	Curing period (days)	7
Steel CA-50		**Stud bolt**	
Modulus of elasticity (kN/cm²)	2.00E+04	Dimension (cm)	2.2 x 20.8
Poisson’s ratio	0.3	Spacing (cm)	50.5
Yield stress (kN/cm²)	32	Parameter "a" (kN)	130
		Parameter "b" (1/cm)	12

2.2 Bridge model

The model for the bridge was based on the validation of the composite beam model presented in Schmitz (2017). Because of the symmetry in the transverse section it was defined the use of this symmetry on the model, thus only one half of the transverse section was modeled considering symmetry conditions. Other restrictions applied on the model are due the end supports, it was limited the displacement on directions Y, Z and in one extremity it was limited also the displacement on direction X.

Mesh options was justified by previous analysis on composite beams, but considering the dimensions of the structure it was done a short investigation about the slab FE mesh, verifying the response of stresses considering the self weight of the structure. The aspect of the mesh used in the next analysis is presented in Fig. 9. It was adopted along the span one element between two connectors. In Fig. 9, the conditions represented in green are the coupled nodes that form the connectors. About the reinforcement bars it is important to say that it was adopted a distribution more uniform to facilitate the modelling process, but it was respected a similar area of steel.

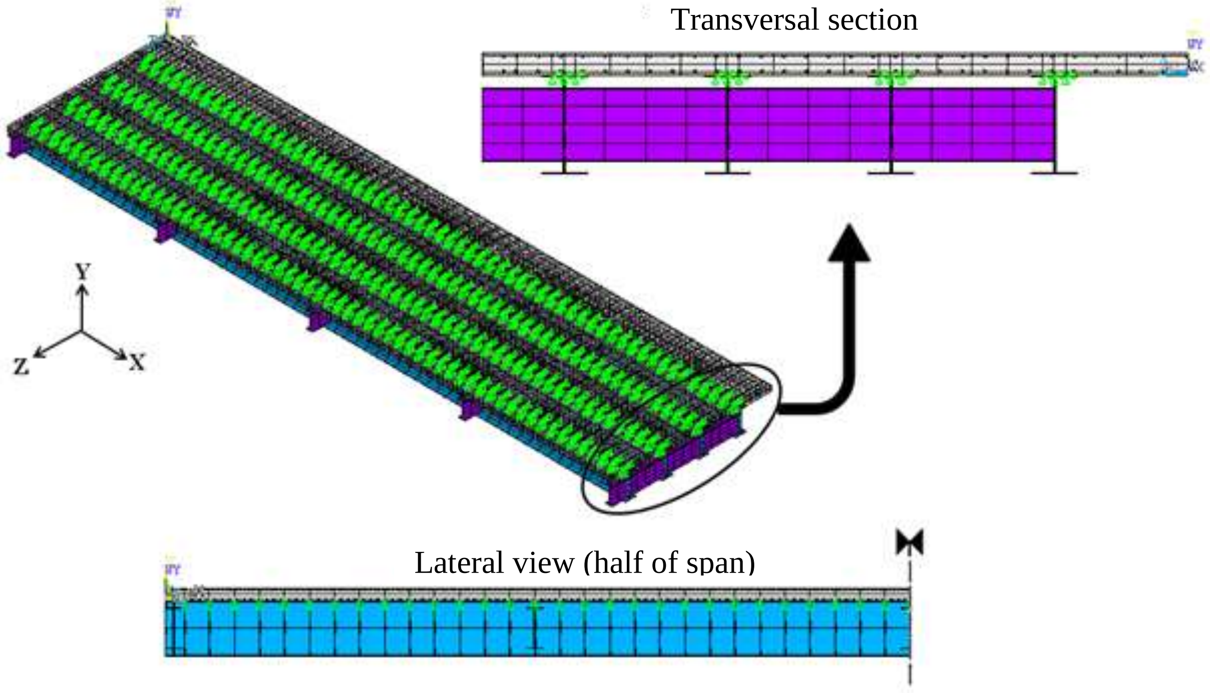

Figure 9. Model of the analyzed bridge

2.3 Study of deferred effects

The first analysis was about the creep and shrinkage effects considering only the permanent loads, in this case: the self weight of the structure and the weight of the barrier and asphalt. For the period of analysis was chosen ten years (3650 days), imagining that on this period had occurred the most important deformation generated by these effects. It is known the influence of the environmental conditions on these phenomena, so intended to analyze some different situations it was defined three temperatures and three values for air humidity. These environmental conditions are combined, generating 9 situations for analysis, that was analyzed by two codes: Comité Euro-International du Béton (1993) – CEB-FIP90 and Féderation Internationale du Béton (2012) – FIB2010.

Figs. 10 and 11 showed the obtained results for CEB-FIP90 and FIB2010, respectively, of middle span of the more externally beam, because it has demonstrated the most severe deformation. The first observation is that the FIB2010 gives a more severe condition after 10 years, despite the group of curves demonstrate the same behavior: same shape, biggest grow of deflection on the beginning and trend to stabilize along the time. As imagined, the increase of temperature represents a increase in creep and shrinkage effects, generating a bigger deflection. In the same way, the decrease of air humidity increases the drying process, generating a bigger deflection. Maybe because the range of the chosen values for temperature and humidity, the change of humidity for a same temperature generates more impact than the change of temperature for a same air humidity.

The maximum deflection was between 9.67 cm and 12.4 cm for FIB2010, and for CEB-FIP90 the variation was between 8.83 cm and 11.63 cm. It is important to highlight that the conditions were constants in ten years of analysis, and normally there is variation on the environmental conditions. The worst condition was 27 °C and 50% of air humidity by FIB2010. So this condition was considered for the next analysis.

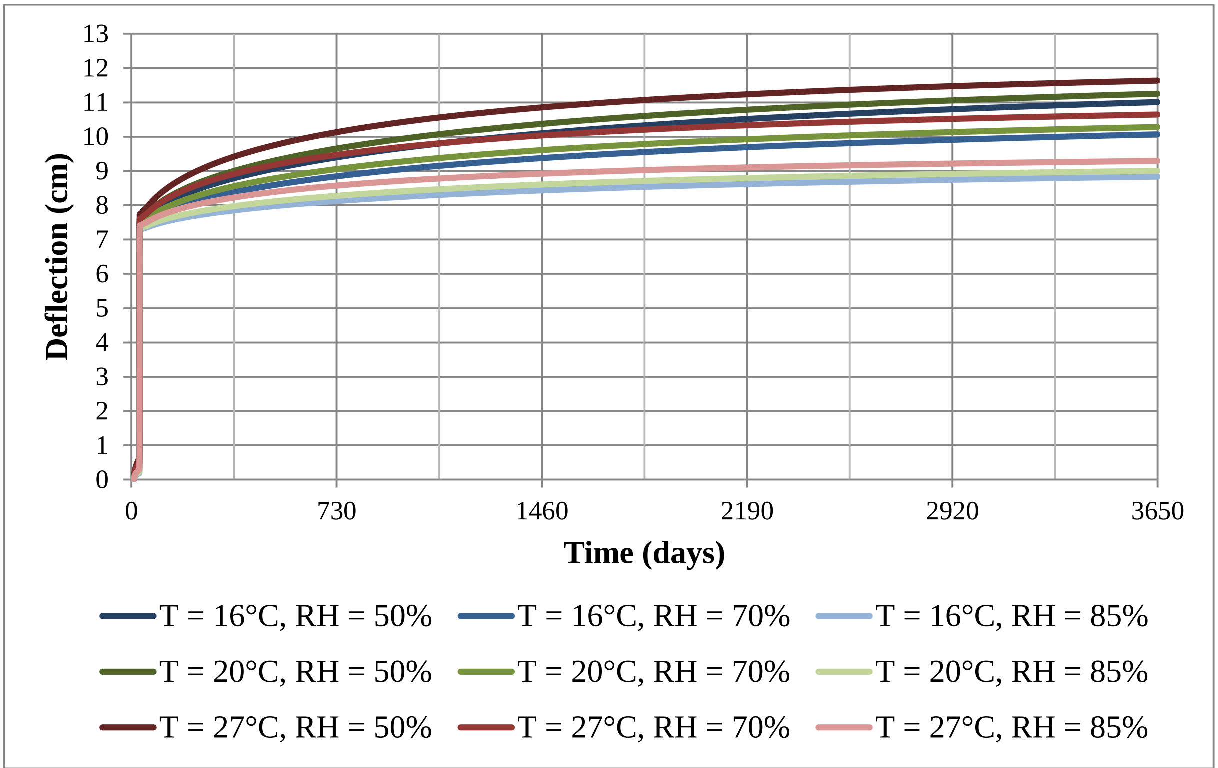

Figure 10. Maximum deflection along the time - CEB-FIP90

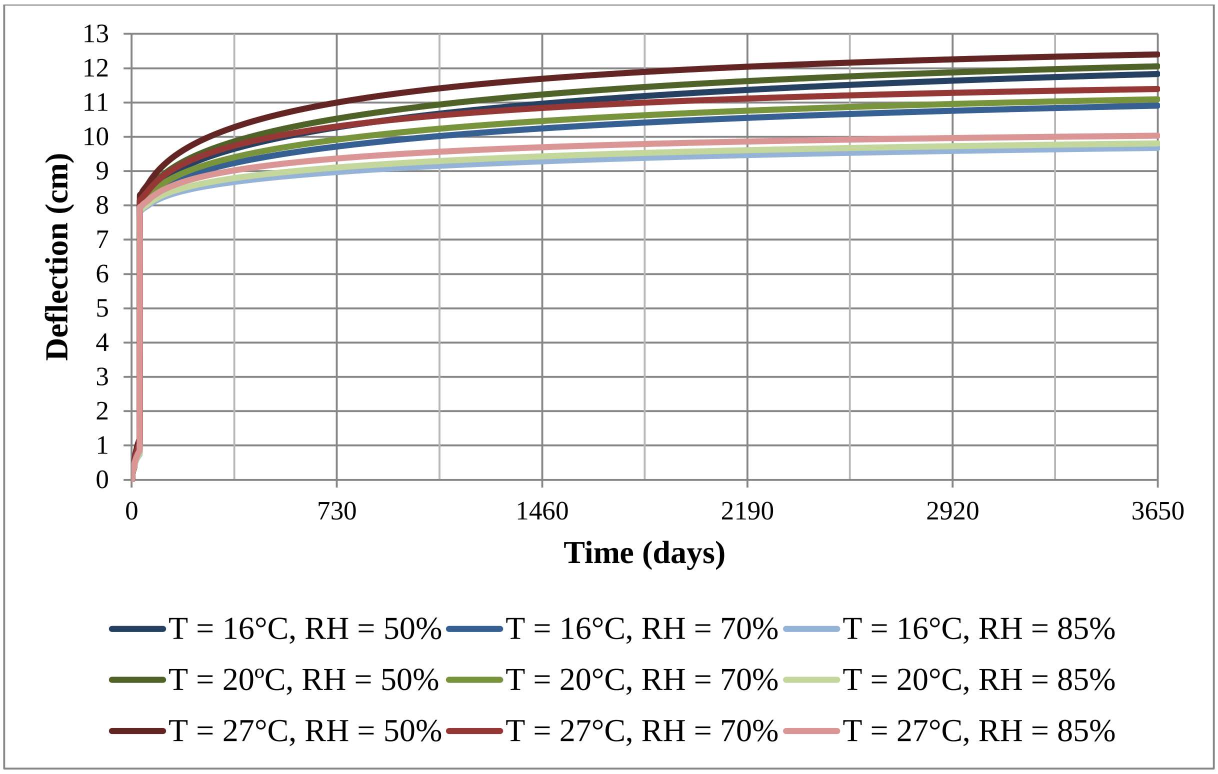

Figure 11. Maximum deflection along the time - FIB2010

Thinking about how the deflection occur along the time, it was analyzed the worst situation, considering the increment of total deformation, assessing the increment of vertical displacement. In Fig. 12, it is possible to verify that the increment has the bigger value when the weight is considered (28 days) and then creep and shrinkage have an important influence on the structure. The increment of deflection tends to zero for infinite time, but even to a time not so high, it is possible to understand that the increment, even no being zero, has so low value that does not generate important consequences on the structure. Therefore, looking the Fig. 12 it is verified that more than 90% of the deformation occur until the first 5 years. So the analysis until this age gives a good prediction of deformation generated by deferred effects.

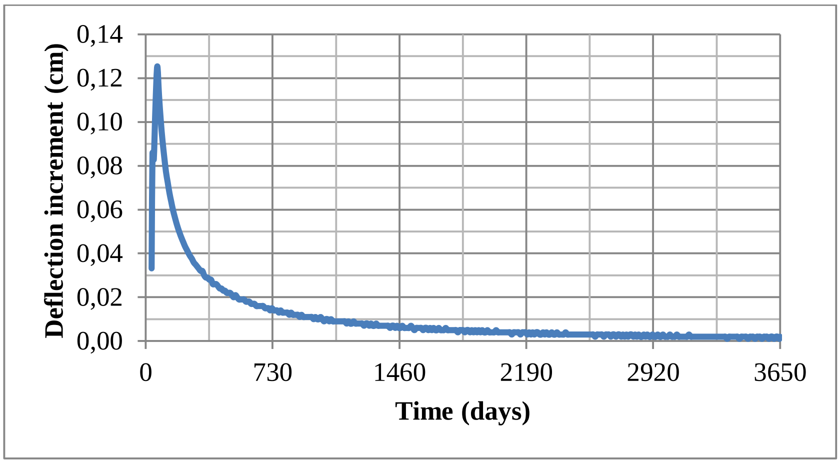

Figure 12. Increment of deflection on the middle span for the most externally beam

Proceedings of the XXXVIII Iberian Latin-American Congress on Computational Methods in Engineering
P.O. Faria, R.H. Lopez, L.F.F. Miguel, W.J.S. Gomes, M. Noronha (Editores), ABMEC, Florianópolis, SC, Brazil, November 5-8, 2017.

Still analysing the same situation it is intersting to verify the stress distribution. In fact, if the analysis is in a concrete element only, the idea is that the stresses will being constant and the deformation grows, considering that no new load will be applied. If the strucuture is only in steel, normally it does not consider deferred effects because they are not significant. But in a composite strucuture the different materials interact, the concrete tends to deform and the steel does not tend to deform, restricting the deformation of the slab.

The more interesting result about stress distribution is presented in Fig. 13, which presents the stress σ_{xx} (kN/cm²) on the two extremes dates, 28 days and 3650 days. At 28 days there is a small tension that occur near the supports, which is expect. But at 3650 days the distribution of this stress changes, it comes up tension on the region in contact with the four "I" profiles, and it is clearly defined. Another important verification is that the level of tension increase significantly, considering that the resistance in tension is around 0.38 kN/cm², probably the regions around the studs bolt are cracking. About the process of cracking it can not evaluated because this analysis is around the viscoelastic behavior and the cracking is not contemplated on this model.

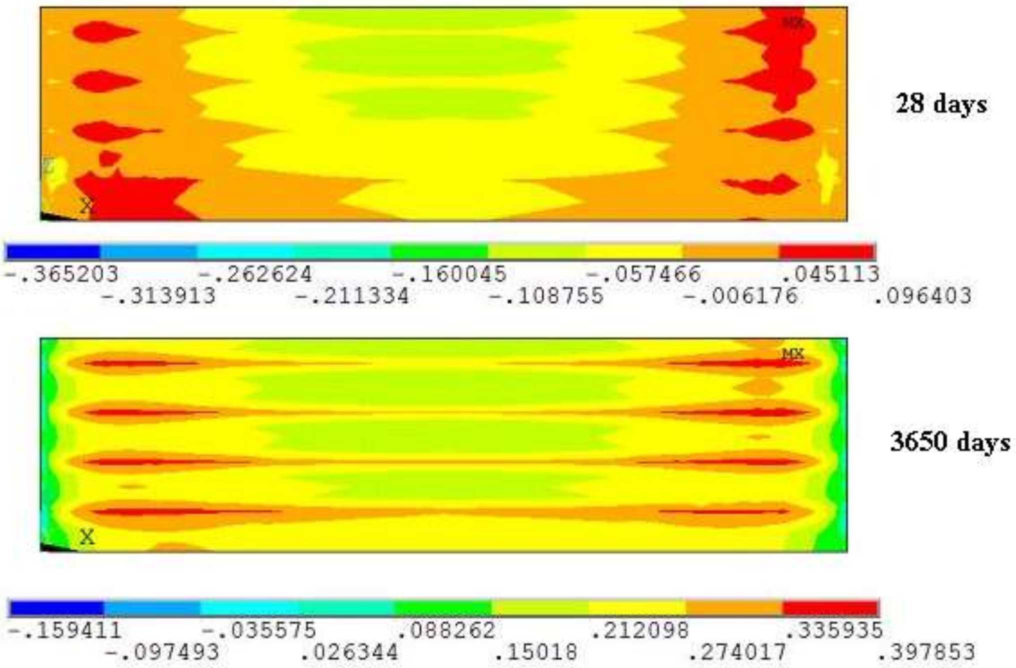

Figure 13. Stresses σ_{xx} (kN/cm²) on the bottom surface of the slab

2.4 Analysis of stress distributions

The analysis of stress distribution considered the bridge with all predicted loads applied, permanents and lives, presented in Table 2, considering the Brazilian normative NBR 7188, by ABNT (2013). Using the loads it was created two situations, the first was a young structure (28 days), disregarding any effect of creep and shrinkage. The second situation was a structure with 10 years in service (3650 days) subjected to the worst environmental condition verified (27 ºC, 50% of air humidity). Therefore, on the second situation was added the effects of shrinkage and creep for the permanent load.

Considering the young structure, by using the post processor of ANSYS, the load effects are combined linearly considering the ultimate limit state, presented on the other Brazilian code, NBR 8681, by ABNT (2003). It is important to explain that the vehicle was considered in the middle of the transverse section and because of the symmetry only half of its weight was considered, and it is the principal live load.

Table 2. Loads acting in the bridge

Type	Load	Direction	Region	Value	
Permanent	Slab own weight	Vertical	–	2.50E-05	kN/cm³
	Beams own weight	Vertical	–	7.70E-05	kN/cm³
	Barriers	Vertical	Between the sidewalk and lane	5.75E-04	kN/cm
	Asphalt	Vertical	lanes	3.92E-04	kN/cm²
Live	Vehicle	Vertical	Until 5m of the ends	94.875	kN/wheel
			Others regions	75.900	kN/wheel
	Traffic (Distributed)	Vertical	Until 5m of the ends	7.906E-04	kN/cm²
			Others regions	6.33E-04	kN/cm²
	Sidewalk	Vertical	sidewalk	3.00E-04	kN/cm²
	Braking/acceleration	Horizontal parallel of span	lanes	135	kN

The level of stress in each part of the beam was different, so to observe them is necessary to look at the of the element separately. In Fig. 14a it is presented the von Mises stresses for the steel beams, including the transverse beams, and the reinforcement. The level of stresses in the trasnverse beam is low, but the use of them was justified by AASHTO (2012), giving a more stability for the structure. The principal beams still in the elastic branch, reaching 96% of the yield stress. Fig. 14b demonstrates that the reinforcement was subjected to low stress levels, and it is also in the elastic behavior.

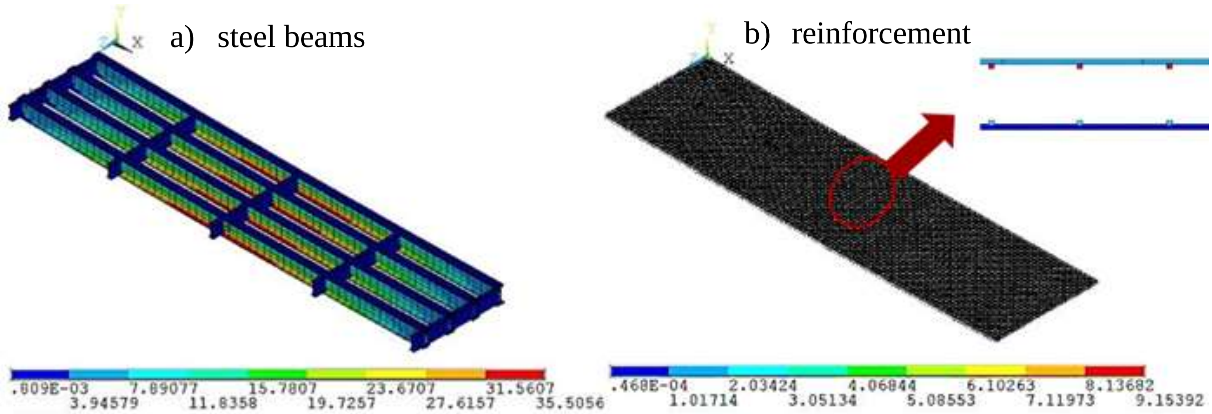

Figure 14. von Mises stresses (kN/cm²) – structure with 28 days a) steel beams b) reinforcement

Observing the slab in Fig. 15, only the concrete, is possible to see the waited behavior, a small tensions on the ends, near the supports. The bigger compression occur in the middle of span and in the middle of transverse section, local of the pontual load of vehicles wheels. Concrete compression is around 38% of your compressive strenght.

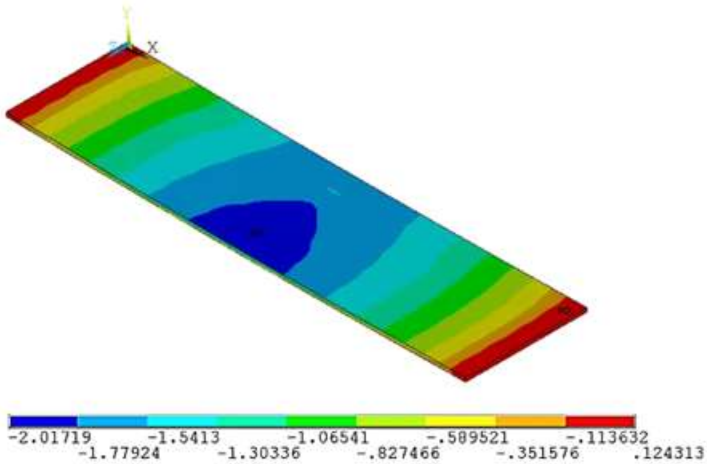

Figure 15. Stresses σ_{xx} (kN/cm²) in concrete slab – structure with 28 days

Still verifying the stress distribution, but now along the composite beam height on middle span. Fig. 16 presents the stresses σ_{xx} in kN/cm² for the most external and most internal beam, considering the x-axis the interface between the slab and the "I" girder. In this way, it is possible to verify the position of the neutral axis. In fact, the neutral axis is an important parameter for the design of composite steel-concrete beams, making it possible to be compared with the design value. The design predicted the plastification of the beam, because the beam has a compact section (no slender), according the classification of ABNT (2008). The two beams evaluated in the model has the same neutral axis. Moreover, in comparison with the design value there as difference of 7 cm between the neutral axis of both evaluated beams. The design disregarded part of the slab that the model indicates being in compression and could have been considered in the resistance of the composite beam.

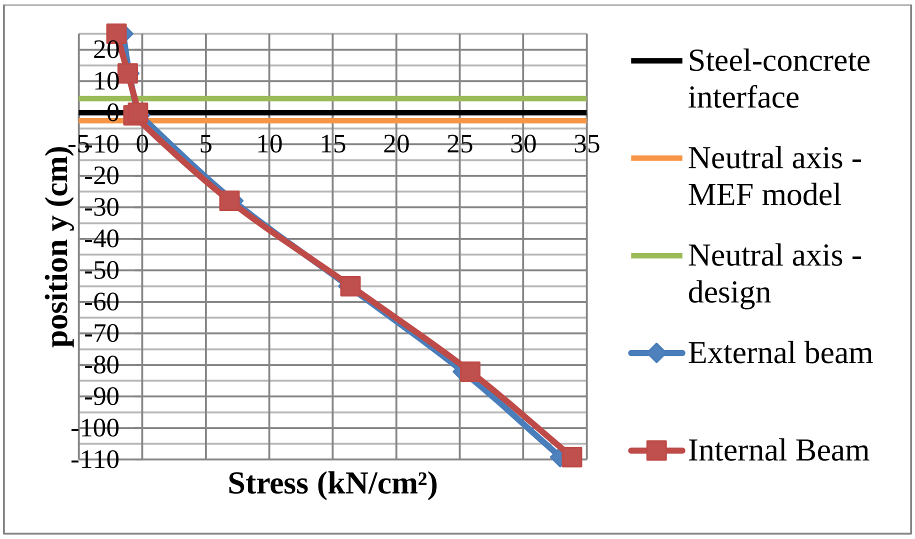

Figure 16. Stress and neutral axis – structure with 28 days

Now considering a structure with 10 years, the permanent load generates creep and also occur shrinkage because of the concrete characteristics. In this case it was combined using again the post processor of ANSYS the permanent load with creep and the shrinkage included with the live loads, being applied the same type of combination. In Fig. 17a are presented the von Mises stress for the steel beams and in Fig.17b the stress for the reinforcemet, and in both elements it was verified an increase of stress. In transverse beams the increase still generates a small level of stress. The steel of the principal beams are in the hardening branch. In the bottom flanges the tension is around 90% of the ultimate stress. Considering that the deferred effects generates deformation on slab and the steel profile tends to contain them, the increase of tension is justified. In the reinforcements it was observed a high increase in the stress level, and in concentrated points in the middle span the steel is near the yield stress.

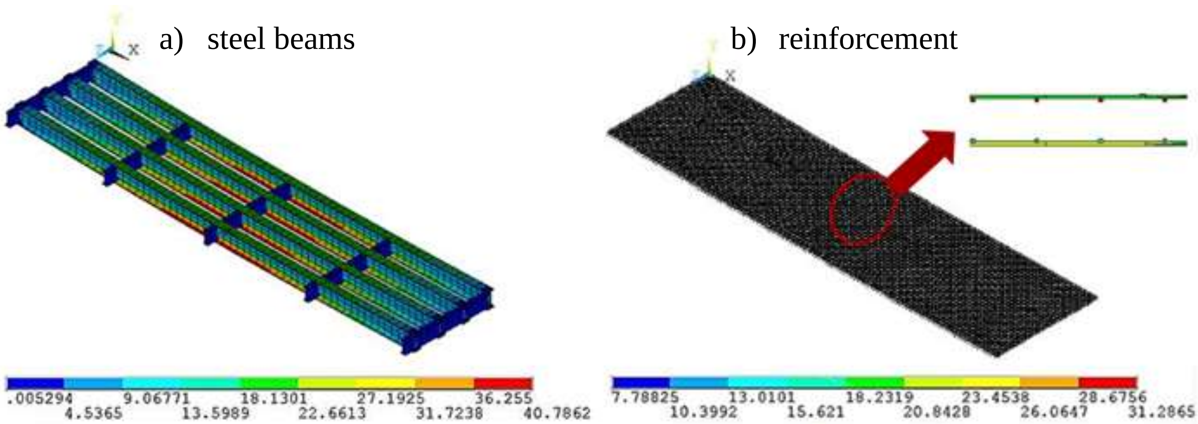

Figure 17. von Mises stresses (kN/cm²) – structure with 3650 days a) in steel beams b) reinforcement

The stress σ_{xx} on concrete slab's had a small increase in compression, but the distribution on the top of the slab is still the same. The important effect observed was the tension significant increase on the bottom of the slab in the connectors region, as presented in Fig. 18. The limit of tension resistance was greatly exceeded. Considering the type of analysis, combining results in post process it was impossible to analyze the cracking. A tentative was done to analyze the structure with deferred effects for the permanent loads and then add the live load for a new analysis. However, the tensions level was high that it was impossible to analyze. This is a consequence of the viscoelastic model programmed that does not verify cracking, so does not correct the tension level when cracking occur. The conclusion is that in the connector region appear tensions on the slab when deferred effects occur. To identify the correct values and see the cracking on this process, is necessary to increment the current program code to analyze cracking also in viscoelastic behavior.

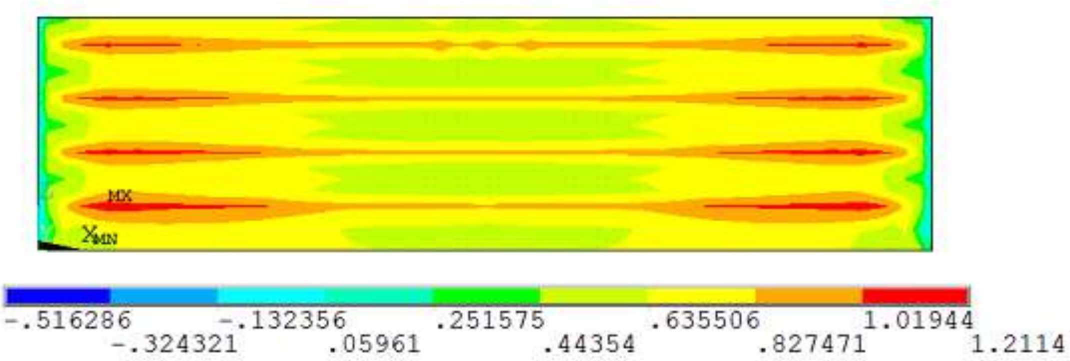

Figure 18. Stresses σ_{xx} (kN/cm²) in concrete slab – structure with 3650 days

Lastly, it was verified the stress distribution along the height of the more internal and more external beams, in order to define the neutral axis. Form Fig. 19 one can verifies that the neutral axis of the two beams are not the same, being present a small difference. Another important verification is related to the discontinuity of stress in the interface region. This occurs because there is a slip in the connectors, that occurs only for severe deformation levels of structure, because they were designed supposing a complete interaction. The change of the neutral axis is attributed to deferred effects that generates an increased region of the steel profile in compression.

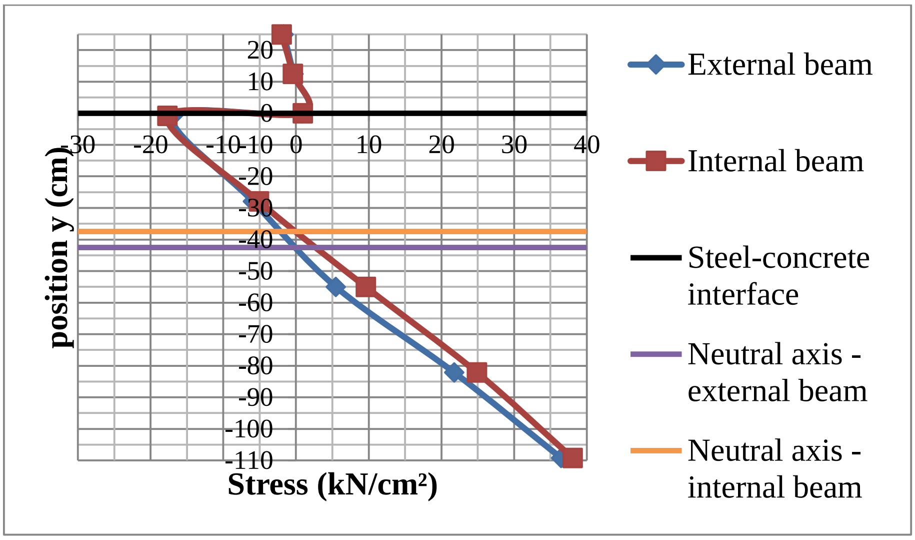

Figure 19. Stress and neutral axis – structure with 3650 days

2.5 Analysis of effective width

Considering the real behavior of a composite structure, the use of shear connectors generates shear stress on the concrete slab, so the distribution of stress along the transverse section is not constant and this effect is known as shear lag. Consequently, when the slab deforms, the section, that was plane, will not be plane anymore. Considering that the sections do not stay planes after the deformation, many simplifications of design can not be used and the design becomes more complex. Therefore, an alternative to analyze the slab, in a more simple way, is considering constant stress. However to make this simplification the width considered on the composite beam can not be the real width, but an effective width. The definition of effective width is the region of the slab that, assuming a constant value for stress, generates the same stress resultant that is acting on the real width.

The intention is to verify the effective width and compare it with the value considered in the design, which was previously of this work. For this, it will be used the definition of Castro et al. (2007), presented in Eq. 4:

$$b_{ef} = \frac{1}{\left[\sigma_{xx}\right]_{y=0}} \int_{-b_c/2}^{+b_c/2} \sigma_{xx}\, dy \tag{4}$$

where $[\sigma_{xx}]_{y=0}$ is the stress σ_{xx} on the axis of the composite beam, b_c is the real width, and σ_{xx} is the stress verified along the transverse section. For this definition it is possible to evaluate the stress at the middle height of the slab or at the top, both are acceptable.

To compare the effective width calculated from the model with the design value is important to make some considerations about the normative calculus. Considering the simply supported structures, according to NBR8800, ABNT (2008), the effective width corresponds to the sum of the distance between outstand shear connectors and the smaller value on each side:

a) distance between the outside connector to a point mid-way between adjacent webs;

b) distance between to the free edge, if there is a part of the slab in cantilever;

c) the span divided by 8.

In fact, although the NBR 8800 does not apply direct to the design of bridges but the EUROCODE 4, European Commitee for Standardization (2005), predicts the same formulation in cases of end supported beams.

Considering the stress distribution and the Eq. 4, it was defined the effective width for the top and middle height of slab, disregarding any deferred effects, that is the structure with 28 days of age. Table 3 presents these values and also a comparison with the code values and the difference percentage. Beam 1 is the most external beam and Beam 4 is the most internal beam. The most difference between normative value and the calculus with the finite elements model was 5.28%, which is considered a relatively small difference.

Table 3. Effective width considering the structure with 28 days

	Beam 1		Beam 2		Beam 3		Beam 4	
	Effective width (m)	Dif. (%)	Effective width (m)	Dif. (%)	Effective width (m)	Dif. (%)	Effective width (m)	Dif. (%)
Middle height	234.26	3.00%	180.63	1.29%	180.74	1.23%	177.80	2.84%
Top	228.75	5.28%	180.22	1.52%	179.23	2.06%	175.70	3.99%
NBR 8800	241.5	-	183	-	183	-	183	-

In order to evaluate how the deferred effects can modify the stress distribution and consequently the effective width, it was verified the stress distribution for the structure with ten years (3650 days). In the investigated structure act a service load, that is the variable load, and the permanent load with the deferred effects of creep and shrinkage. The same environmental situation evaluated in the previous item 2.4. Calculating the effective width, that is present in Table 4 for all beams on the two positions evaluated, it was verified that the effective width changes, but in a not so significant value. In all cases, the effective width have reduced a small value in comparison with the young structure, then, the difference considering the normative value increased to 6.25%. Therefore, the consideration of a same effective width for all structure life is not a bad approximation.

Table 4. Effective width considering the structure with 3650 days

	Beam 1		Beam 2		Beam 3		Beam 4	
	Effective width (m)	Dif. (%)	Effective width (m)	Dif. (%)	Effective width (m)	Dif. (%)	Effective width (m)	Dif. (%)
Middle height	226.41	6.25%	176.49	3.56%	177.43	3.04%	178.11	2.67%
Top	229.16	5.11%	178.10	2.68%	176.19	3.72%	175.26	4.23%
NBR 8800	241.5	-	183	-	183	-	183	-

3 CONCLUSIONS

The present work have presented some analysis in a hypothetic composite steel-concrete bridge, designed with Brazilian normative and some recommendations of other international codes, like EUROCODE 4 and AASHTO. The bridge was modeled in a commercial software of finite elements, ANSYS, considering the validation of a model for composite beam, presented in detail in Schmitz (2017). The models of the materials have made possible the evaluation of short term loads effects and long term loads effects, such as creep and shrinkage.

The first analysis was done considering the bridge in nine different environmental conditions constants along through ten years. The results agreed with the expectative. The worst condition was for the hotter temperature and the smaller air humidity level. Despite the analysis was in ten years, more than 90% of the deferred effects occur in the first five years.

The next verification was comparing the young structure and the structure with ten years on the worst condition verified. The tension level on the I profile demonstrate a good exploitation of the steel, that reach 90% of the ultimate stress in the worst condition. The deformations restriction imposed by the steel profile generates stress tension in the connectors regions of the concrete slab. This indicates cracking in this region, but for correct values further analysis should be done.

About the neutral axis, that was one parameter used in design, the young structure demonstrates that the whole height of slab are in compression and would be considered contributing to the resistance of the composite beam. The design neutral axis was smaller, and part of the slab was desconsidered in the computed resistance. Considering the structure with 10 years, because of the tensions values in connector region it is difficult to define the real compression region in slab. The other important parameter in design, effective width, was also verified. The condition for a young structure demonstrates a maximum difference of 5.28% with the Brazilian normative. Creep and shrinkage effects did not affect significantly the effective width, the difference with the same normative increase to 6.25%. Therefore, the verification with finite elements model demonstrate a good agreement with normative (NBR 8800 and EUROCODE 4), and the difference is attributed to firtly to the simplification in the normative model, that need to be as generic as possible, and secondly, ii) to the imprecisions on the numerical model.

ACKNOWLEDGEMENTS

The authors would like to acknowledge the Brazilians Foundations CAPES and CNPq for the support provided by and the CEMACOM/UFRGS to provide its infrastructure for the development of this work.

REFERENCES

American Association of State Highway and Transport Officials. 2012. *AASHTO LRFD bridge: design specifications*. Washington

ANSYS Inc. *ANSYS Help System*, version 14.5, 2010.

Associação Brasileira de Normas Técnicas. 2003. *NBR 8681: actions and safety of structures – procedure*. Rio de Janeiro.

_____.2008.*NBR 8800: design of steel and composite structures for buildings*. Rio de Janeiro.

_____. 2013. *NBR 7188: road and pedestrian live load on bridges, viaducts, footbridges and other structures*. Rio de Janeiro.

Bazant, Z. P., Prasannan, S. 1988. Solidification theory for aging creep. *Cement and concrete research*, v. 18, n. 6, pp. 923-932.

Castro, J. M., Elghazouli, A. Y., Izzuddin, B. A. 2007. Assessment of effective slab widths in composite beams. *Journal of Constructional Steel Research*, v. 63, pp. 1317-1327.

Comité Euro-International du Béton. 1993. *CEB-FIP Model code 1990*. Lausanne.

Dias, M. M., Tamayo, J. L. P., Morsch, I. B., Awruch, A. M. 2015. Time dependent finite element analysis of steel-concrete composite beams considering partial interaction. *Computers and Concrete*, v. 15, n. 4, pp. 687-707.

European Commitee for Standardization. 2005.*Eurocode 4 – design of composite steel and concrete structures – part 2: general rules and rules for bridges*. Brussels.

Féderation Internationale du Béton. 2012. *FIB-2010 Model code 2010*. Lausanne, Bulletin n. 65.

Gattesco, N. 1999. Analytical modeling of nonlinear behavior of composite beams with deformable connection. *Journal of Constructional Steel Research*, v. 52, pp. 192-218.

Kotinda, Y. J. 2006. *Numerical modeling of steel-concrete composite beams simply supported: emphasis to the study of the slab-beam interface* (in Portuguese). M.Sc. Thesis, University of Sao Paulo/São Carlos.

Martinelli, M. 2003. *Modelling situations of punching on reinforced concrete slab through the elements finite method* (in Portuguese). M. Sc. Thesis, Federal University of Rio Grande do Sul/Porto Alegre.

Moreno, J. C. A. ;Tamayo, J. L. P. ; Morsch, I. B. ; Dias, M. M. ; Calderon, W. R. 2016. Influence of Creep and Shrinkage Models in the Long-term Behavior of Steel-concrete composite beams. In: SMEC 2016 –*Simposio Nacional en Mecánica de Materiales y Estructuras Continuas: Experimentación, Modelado Numérico y Teórico*, v. 1. pp. 1-19.

Queiroz, F. D., Vellasco, P. C. G. S., Nethercot, D. A., 2007.Finite element modelling of composite beams with full and partial connection. *Journal of Constructional Steel Research*, vol. 63, pp. 505-521.

Schmitz, R. J. 2017. *Composite steel-concrete structures*: analysis of a bridge composed by *I* girders (in Portuguese). M. Sc. Thesis, Federal University of Rio Grande do Sul/Porto Alegre.

Tamayo, J., Morsch, I. B., Awruch, A.M. 2015. Short-time numerical analysis of steel-concrete composite beams. *Journal of the Brazilian Society Mechanical Sciences and Engineering*, vol. 37, n. 4, pp. 1097-1109.